(2)

SEC

ORT DOCUMENTATION PAGE

1a. AD-A203 126

1b. RESTRICTIVE MARKINGS

2a.

3. DISTRIBUTION/AVAILABILITY OF REPORT

Approved for public release; distribution unlimited.

2b. DECLASSIFICATION/DOWNGRADING SCHEDULE

4. PERFORMING ORGANIZATION REPORT NUMBER(S)

Prop.No. 22413-CH
Grant No. DAAG29-85-K-0041

5. MONITORING ORGANIZATION REPORT NUMBER(S)

ARO 22413.5-CH

6a. NAME OF PERFORMING ORGANIZATION

University of Pittsburgh

6b. OFFICE SYMBOL (If applicable)

7a. NAME OF MONITORING ORGANIZATION

U. S. Army Research Office

6c. ADDRESS (City, State, and ZIP Code)

Dept. of Chemistry
Pittsburgh, PA 15260

7b. ADDRESS (City, State, and ZIP Code)

P. O. Box 12211
Research Triangle Park, NC 27709-2211

8a. NAME OF FUNDING/SPONSORING ORGANIZATION

U. S. Army Research Office

8b. OFFICE SYMBOL (If applicable)

9. PROCUREMENT INSTRUMENT IDENTIFICATION NUMBER

DAAG29-85-K-0041

8c. ADDRESS (City, State, and ZIP Code)

P. O. Box 12211
Research Triangle Park, NC 27709-2211

10. SOURCE OF FUNDING NUMBERS

PROGRAM ELEMENT NO.	PROJECT NO.	TASK NO.	WORK UNIT ACCESSION NO.

11. TITLE (Include Security Classification)

Flow Reactor Studies of Elementary Radical Reaction Rates

12. PERSONAL AUTHOR(S)

Michael F. Golde

13a. TYPE OF REPORT	13b. TIME COVERED	14. DATE OF REPORT (Year, Month, Day)	15. PAGE COUNT
Final	FROM 2/14/85 TO 8/13/88	12/5/88	28

16. SUPPLEMENTARY NOTATION

The view, opinions and/or findings contained in this report are those of the author(s) and should not be construed as an official Department of the Army position, policy, or decision, unless so designated by other documentation.

17. COSATI CODES		
FIELD	GROUP	SUB-GROUP

18. SUBJECT TERMS (Continue on reverse if necessary and identify by block number)

Chemical kinetics; elementary reactions; methoxy radicals; discharge-flow.

19. ABSTRACT (Continue on reverse if necessary and identify by block number)

The kinetic behavior of several elementary gas-phase reactions has been studied using the discharge-flow technique. Detection techniques include resonance fluorescence, laser-induced fluorescence and mass spectrometry. The rate of the reaction of H atoms with O_2 to form HO_2 has been determined over the temperature range 298 to 639K, with He, N_2, and H_2O as third bodies. The third order rate constants are

$$k^{III}(He) = (4.0\pm1.2) \times 10^{-33}\exp[(560\pm100)/T] \text{ cm}^6\text{s}^{-1}$$

$$k^{III}(N_2) = (6.5\pm2.2) \times 10^{-33}\exp[(680\pm110)/T] \text{ cm}^6\text{s}^{-1}$$

$$k^{III}(H_2O) = (1.9\pm0.9)\times10^{-32}\exp[(1050\pm140)/T] \text{ cm}^6\text{s}^{-1}$$

20. DISTRIBUTION/AVAILABILITY OF ABSTRACT

☐ UNCLASSIFIED/UNLIMITED ☐ SAME AS RPT. ☐ DTIC USERS

21. ABSTRACT SECURITY CLASSIFICATION

Unclassified

22a. NAME OF RESPONSIBLE INDIVIDUAL	22b. TELEPHONE (Include Area Code)	22c. OFFICE SYMBOL

DD FORM 1473, 84 MAR

83 APR edition may be used until exhausted. All other editions are obsolete.

SECURITY CLASSIFICATION OF THIS PAGE

UNCLASSIFIED

19. ABSTRACT (continued)

The efficiency of CH_3O formation in the reactions of F and OH radicals with CH_3OH has been probed via product studies of the former reaction and via rate constant measurements of several isotopic variants of the latter reaction. Values of the branching fraction for CH_3O formation of respectively 0.75±0.10 and 0.15±0.08 were obtained. Rate constants of the CH_3O + NO reaction have been measured over a range of pressure and temperature. For the combination channel, the limiting low pressure rate constant is deduced to be $(2.9\pm0.3) \times 10^{-29}(T/300)^{-2.5\pm1.0}$ cm^6s^{-1}; for the bimolecular abstraction channel (yielding CH_2O + HNO), the value is $(7.9\pm1.0) \times 10^{-13}\exp[(400\pm40)/T]$ cm^3s^{-1}. The products of both channels have been detected, establishing that atom transfer is the major channel at low pressure.

Initial measurements suggest that the reaction of CH_3O with H atoms is extremely fast, $k \sim 1 \times 10^{-10}$ cm^3s^{-1}; the reaction of CH_3O with O atoms is significantly slower, with $k \sim (3\text{-}10) \times 10^{-12}$ cm^3s^{-1}.

Keywords: -> to fig. 2 18

19. ABSTRACT (continued)

The efficiency of CH_3O formation in the reactions of F and OH radicals with CH_3OH has been probed via product studies of the former reaction and via rate constant measurements of several isotopic variants of the latter reaction. Values of the branching fraction for CH_3O formation of respectively 0.75±0.10 and 0.15±0.08 were obtained. Rate constants of the CH_3O + NO reaction have been measured over a range of pressure and temperature. For the combination channel, the limiting low pressure rate constant is deduced to be $(2.9\pm0.3) \times 10^{-29}(T/300)^{-2.5\pm1.0}$ cm^6s^{-1}; for the bimolecular abstraction channel (yielding CH_2O + HNO), the value is $(7.9\pm1.0) \times 10^{-13}\exp[(400\pm40)/T]$ cm^3s^{-1}. The products of both channels have been detected, establishing that atom transfer is the major channel at low pressure.

Initial measurements suggest that the reaction of CH_3O with H atoms is extremely fast, $k \sim 1 \times 10^{-10}$ cm^3s^{-1}; the reaction of CH_3O with O atoms is significantly slower, with $k \sim (3\text{-}10) \times 10^{-12}$ cm^3s^{-1}.

Keywords: → to field 18

Accesion For	
NTIS CRA&I	☑
DTIC TAB	☐
Unannounced	☐
Justification	
By	
Distribution /	
Availability Codes	
Dist	Avail and / or Special
A-1	

1. Introduction

Most reactions between stable molecules in the gas phase occur via a sequence of simple reaction steps, involving highly reactive radicals. Knowledge of the rates and products of such elementary reactions are needed for successful modeling of any complex reaction system, including those in the natural and perturbed atmosphere and combustion and laser systems. While much is known about reactions involving H-atom abstraction, which includes reactions of e.g. H, O, OH and Cl with stable molecules, reactions occurring via a strongly-bound intermediate are much less well characterized. A major aspect of this project was to obtain reliable rate constants for the combination reaction:

$$H + O_2 + M \rightarrow HO_2 + M \qquad (1)$$

over a wide range of temperature and for several third bodies, for use in modeling combustion systems. Following this study, attention turned to the formation and reactions of the CH_3O radical, as a continuation of a previous study of its reaction with NO_2.[1] The reactions of OH and F with CH_3OH were examined as sources of CH_3O and showed interesting contrasts in behavior. The reaction of CH_3O with NO was studied in detail, via rate constant measurements over a range of pressure and temperature and an investigation of two product channels. A study of the reactions of CH_3O with O and H atoms was commenced; both reactions appear to be very fast. Each of these systems is described further below.

The grant was originally awarded to Professor F. Kaufman (d. July 1985). For the remainder of the grant period, Professor M. Golde acted as principal investigator. The other personnel involved were Dr. J. L. Durant (post-doctoral associate and research assistant professor) and the following graduate students:

K-J. Hsu (Ph.D. 1986), J. A. McCaulley (Ph.D. 1987), N. Kelly (M.Sc. 1986) and A. M. Moyle.

2. Experimental Techniques

Most of the studies were carried out in two discharge-flow apparatuses. One system (system "A")[2] was designed specifically for the relatively high pressures needed for the H + O_2 study and was operated in the range 4 - 70 Torr, with He as the principal carrier gas. H atoms were produced initially via a thermal dissociator. When studying reaction (1) at elevated temperatures, however, the large background of undissociated H_2 participated significantly in interfering secondary reactions. For such studies, the thermal dissociator was replaced by a conventional microwave discharge, which achieved much higher fractional dissociation of the H_2 and thus permitted use of much lower H_2 concentrations. The H-atom stream in He carrier gas was added to the main carrier gas, which consisted either of pure He or mixtures of N_2 (mole fraction 0.27 - 0.74) or H_2O (mole fraction 0.049 - 0.26). O_2 was added further downstream through a movable inlet.

At the downstream end of the flow tube, the gas was expanded via a 0.35 mm diameter orifice into a lower-pressure detection chamber. The principal detection technique was atomic resonance fluorescence, for relative concentration measurements of the H atoms. Another detection port allowed simultaneous detection of OH (and of HO_2 by chemical conversion to OH) by molecular resonance fluorescence.

For experiments at elevated temperatures, a heating mantle encasing the flow tube was used. To minimize wall loss of radicals, the flow tube was coated with halocarbon wax. Above 370K, melting of the wax prevented its use and the tube was rinsed with HF and distilled H_2O. Wall loss rates under these

conditions were very small, $< 3\ s^{-1}$ for H atoms and $\sim 15\ s^{-1}$ for OH radicals.

The other discharge-flow apparatus ("B")[3] operates at normal pressures, 0.5 - 5 Torr with He or Ar carrier gas. Radicals are produced either by pulsed infra-red multi-photon dissociation of precursor molecules, or by microwave discharge of suitable gases followed by rapid chemical conversion to the species of interest. The latter method was used for the studies described here. Three detection techniques are available with this system. Firstly, resonance-fluorescence has been used for detection of OH radicals and of H atoms (by chemical conversion to OH). Secondly, laser-induced fluorescence (Lambda-Physik EMG103MSC, FL 2001) is used for detection of OH and CH_3O and deuterated analogs. Finally, molecular-beam-sampled mass spectrometry is used for characterization of reaction products, including HF, DF and CH_3ONO.

All kinetic measurements were performed under pseudo first-order conditions. The exponential decay of the minor species was monitored as a function of reaction time to yield the effective first order rate coefficient. Runs were repeated over a range of concentrations of the major species to yield the second-order rate constant. Standard corrections were applied where necessary for wall loss and for radial or axial diffusion effects.

3. $H + O_2 + M$

The reaction between H and O_2 can occur via two channels:

$$H + O_2 + M \rightarrow HO_2 + M \qquad (1)$$

$$H + O_2 \rightarrow OH + O \qquad (2)$$

The rates of these channels have widely different temperature dependences and competition between them helps determine the second explosion limit of the H_2/O_2

reaction. The aim of the present study was to obtain reliable data over the temperature range 298 to 1000K, in order to bridge the gap between previous low temperature (200-400K) and high temperature (>950K) studies. He (the main bath gas), N_2 and H_2O were examined as third bodies, M.

Under all conditions, the concentration relationship [M] >> $[O_2]$ >> [H] was maintained. Briefly, the decay of [H] as a function of reaction time yielded an effective first order rate coefficient, k^I. Values of k^I, measured as a function of $[O_2]$, yielded a second-order rate constant, k^{II}. k^{II} was determined at several values of [M] to yield the true third-order rate constant, k^{III}, of reaction (1).

In practice, the plots of k^I vs $[O_2]$ were not accurately linear, due to the effect of secondary reactions initiated by:

$$H + HO_2 \rightarrow OH + OH \quad (3)$$

$$\rightarrow H_2O + O \quad (4)$$

$$\rightarrow H_2 + O_2 \quad (5)$$

for which the branching fractions, f, are respectively 0.87 ± 0.04, 0.04 ± 0.02 and 0.09 ± 0.04.[4] At each value of [M], a mechanism comprising 10 reaction steps was analyzed,[2] with k^{II} varied to obtain the best fit to the experimental k^I. An example of the experimental and calculated k^I is shown in Figure 1. Plots of the resulting k^{II} as a function of [M] for M = He, N_2 and H_2O are shown in Figures 2-4. The k^{III} values obtained were 10-50% lower than those derived by neglecting secondary chemistry.

The study of the H + O_2 reaction at elevated temperatures followed a similar procedure. As the temperature is increased, atom transfer to yield OH + O becomes increasingly important, and it was concluded that, above about

700K, the observed H-atom decay is dominated by this channel, rather than by the combination channel, even at the highest total pressure, 70 Torr, attainable in this system. The study was, therefore, terminated at ~640K.

Our measurements yielded the following third-order rate constants at 298K:

$k^{III}(M = He) = (2.6 \pm 0.2) \times 10^{-32}$ cm^6s^{-1}

$k^{III}(M = N_2) = (6.1 \pm 0.9) \times 10^{-32}$ cm^6s^{-1}

$k^{III}(H_2O) = (6.4 \pm 0.8) \times 10^{-31}$ cm^6s^{-1}.

Over the temperature range 298 - 639K, we determined:

$k^{III}(He) = (4.0 \pm 1.2) \times 10^{-33} \exp[(560 \pm 100)/T]$ cm^6s^{-1}

$k^{III}(N_2) = (6.5 \pm 2.2) \times 10^{-33} \exp[(680 \pm 110)/T]$ cm^6s^{-1}

$k^{III}(H_2O) = (1.9 \pm 0.9) \times 10^{-32} \exp[(1050 \pm 140)/T]$ cm^6s^{-1}.

The data at room temperature agree well with several earlier investigations.[5-7] In other studies, incorrect assumptions concerning the rates of secondary reactions were made; reanalysis, using currently-available rate data, yields values close to those presented here. Averaging the available data, we propose the following rate constants at 298K:

$k^{III}(He) = (2.5 \pm 0.1) \times 10^{-32}$ cm^6s^{-1}

$k^{III}(N_2) = (6.3 \pm 0.7) \times 10^{-32}$ cm^6s^{-1}

$k^{III}(H_2O) = (6.3 \pm 0.8) \times 10^{-31}$ cm^6s^{-1}.

The complete set of the present data is plotted in Arrhenius form in Figure 5, together with previous high temperature values. Such data for M = Ar cluster

closely around the extrapolation of the present data for M = He, consistent with the similar M-efficiencies of He and Ar at room temperature. The rates for N_2 are somewhat smaller than extrapolation of the present data, but the ratio $k^{III}(N_2)/k^{III}(Ar)$ determined at 1050K by Slack[8] agrees well with our prediction. The discrepancies in the literature values for $k^{III}(H_2O)$ at high temperature[9,10] prevent a critical comparison with an extrapolation of the present data. In summary, the present data have established that the room temperature and high temperature data can be bridged via Arrhenius expressions for the rate constants.

The data show H_2O to be a much more efficient third body than either He or N_2. This is ascribed to the greater efficiency of H_2O at stabilizing the initially-formed hot HO_2^* species via energy transfer in collisions; this M effect has been observed previously in several other combination reactions. As the temperature is raised, the difference in M efficiencies of He and H_2O decreases somewhat.

4. The Reactions of F and OH with CH_3OH.

These reactions were initially investigated in order to assess their potential as sources of methoxy radicals, CH_3O; however, they were found to be sufficiently interesting to warrant a more extended study. In each reaction, H-atom abstraction from either end of the CH_3OH molecule is possible, but with different exothermicities:

$$OH + CH_3OH \rightarrow H_2O + CH_3O + 15.6 \text{ kcal/mol} \quad (6)$$

$$\rightarrow H_2O + CH_2OH + 25.3 \text{ kcal/mol} \quad (7)$$

$$F + CH_3OH \rightarrow HF + CH_3O + 32.8 \text{ kcal/mol} \quad (8)$$

$$\rightarrow HF + CH_2OH + 42.5 \text{ kcal/mol} \quad (9)$$

In the first reaction, it has been found that the more exothermic channel is strongly favored. However, the product distribution from the second reaction, which occurs at close to the collision rate, is very uncertain, literature values for the branching fraction for the channel leading to CH_3O ranging between 0.3 ± 0.1 and 0.63 ± 0.07 (See Table 1). In the present study, the branching fraction for this reaction was investigated by a more direct method than those used previously; and the rate constants of several isotopic variants of the OH + CH_3OH reaction were determined at room temperature, yielding new insight into this reaction.

Channels (8) and (9) were investigated by mass spectrometry in apparatus "B" by comparing the yields of HF and DF from the reactions of F with CH_3OD or CD_3OH, e.g.

$$F + CH_3OD \rightarrow HF + CH_2OD \quad (10)$$

$$\rightarrow DF + CH_3O \quad (11)$$

Signals at m/e 20(HF) and 21(DF) were measured over a concentration range, [methanol]/[F], of 2 to 80, a total carrier gas pressure of 0.5 - 2 Torr and with both wax-coated and uncoated flow tubes. Consistent results were obtained, yielding branching fractions for methoxy formation of 0.81 ± 0.07 from CH_3OD and 0.69 ± 0.08 from CD_3OH. This difference is not considered significant and it is concluded that kinetic isotope effects are quite small for this reaction, in agreement with previous findings.[11,12] This is confirmed by a very recent study,[11] which additionally finds a CH_3O branching fraction of ~ 0.62, in support of our value. The branching fractions are summarized in Table 1.

In the OH + CH_3OH study, OH (OD) was formed by the rapid reaction of H (D) with NO_2, and detected by laser-induced fluorescence using the $OH(A^2\Sigma^+ - X^2\Pi)$

transition. Concentration ratios, [methanol]/[hydroxyl], were kept sufficiently large for possible secondary reactions of OH with reaction products to be unimportant.

Measured bimolecular rate constants for 7 isotopic variants of the OH + CH_3OH reaction are summarized in Table 2. The value for OH + CH_3OH itself agrees well with previous data. No other data for the reactions of the deuterated species appear to be available. Deuteration of the methyl group causes a large decrease in the rate constants, while deuteration of the hydroxyls has a much smaller effect. If it is assumed that primary isotope effects (i.e. in the bond to be broken) are much larger than secondary effects due to substitution in other bonds, then the results imply that channel (7) predominates over (6), and a simple model[13] yields a branching fraction of 0.15 ± 0.08 for CH_3O formation in the OH + CH_3OH reaction, in good agreement with earlier measurements.

It is concluded that the branching in the reactions of F and OH with CH_3OH differs markedly, with the rapid F reaction (which has a negligible activation energy) strongly favoring the less exothermic channel. It is interesting that both UV photodissociation of CH_3OH and the reaction of electronically-excited N_2 in the ($A^3\Sigma_u^+$) state with CH_3OH also favor cleavage of the CH_3O-H bond. In contrast, H-CH_2OH cleavage is dominant in the reaction of Cl with CH_3OH; however, abstraction of the hydroxyl H atom is endothermic in this case.

3. Investigation of the reaction CH_3O + NO.

This reaction is of possible importance in polluted atmospheres and is of direct relevance to the decomposition of CH_3ONO, a model propellant. The reaction is of interest as it offers the possibility of two competing channels:

$$CH_3O + NO \xrightarrow{M} CH_3ONO \quad (12)$$

$$\rightarrow CH_2O + HNO \quad (13)$$

The latter channel may occur via two possible mechanisms: either direct abstraction of H from CH_3O, or unimolecular decomposition of the intermediate CH_3ONO. We have measured the second-order rate constant of the overall reaction over the pressure range (M = He, Ar) 0.75 - 5 Torr and the temperature range 223 - 473K. The reaction products have been examined over a smaller range of conditions. For the kinetic measurements, CH_3O radicals were produced by two separate reactions:

(i)
$$F + CH_4 \rightarrow CH_3 + HF \quad (14)$$

$$CH_3 + NO_2 \rightarrow CH_3O + NO \quad (15)$$

(ii)
$$F + CH_3OH \rightarrow HF + CH_3O \quad (16)$$

In each case, F atoms were produced by discharging a dilute mixture of F_2 in He. CH_3O was detected by LIF in the ($A^2A_1 - X^2E$) band system, utilizing lines in the 3_0^2 band at 303.8 nm. Initial concentrations of CH_3O in the reaction zone were typically $< 5 \times 10^{11}$ cm^{-3}.

In the presence of NO, CH_3O decayed exponentially over a concentration range of at least 10, but often flattened out at large reaction times, indicative of a secondary process forming CH_3O radicals. The source was not definitely identified, but heterogeneous processes are suspected. Kinetic data were derived from the linear portions of the plots of $\ell n(I_{LIF})$ vs reaction time. Typical decay curves are shown in Fig. 6, and a plot of the first order rate coefficient vs [NO] in Fig. 7. The resulting second-order rate coefficient

increases slightly with pressure between 1 and 5 Torr, and decreases significantly with increasing temperature between 200 and 450K, as illustrated in Fig. 8.

The products of this reaction were investigated in two ways. CH_3ONO was detected via mass spectrometry at m/e 61 (parent) and 60. The signal was calibrated using pure CH_3ONO. A small correction was applied for CH_3NO_2, detected as a minor product of the $CH_3 + NO_2$ precursor reaction, equ. 15. [It was concluded that the branching fraction for CH_3NO_2 formation was 0.040 ± 0.004 at 0.5 Torr total pressure, and 0.07 ± 0.02 at 1 Torr]. For the $CH_3O + NO$ reaction, the branching fractions for CH_3ONO formation were 0.11 ± 0.02 (0.52 Torr, 298K), 0.20 ± 0.05 (1.0 Torr, 298K) and 0.16 ± 0.05 (1.0 Torr, 223K).

A brief search for HNO, a product of the other channel of this reaction, equ. 13, was not successful in this apparatus. Therefore, the reaction was studied in another flow system, with CH_3O formed by the reaction:[14]

$$N_2^*(A^3\Sigma_u^+) + CH_3OH \rightarrow N_2 + CH_3O + H, \quad f = 0.9 \pm 0.1 \qquad (17)$$

HNO was readily detected via LIF in the ($A^1A'' - X^1A'$) band system. The signal was compared with that from the reaction sequence:

$$N_2^*(A) + CH_2O \rightarrow N_2 + CHO + H, \quad f \sim 1.0 \qquad (18)$$

$$CHO + NO \rightarrow HNO + CO. \qquad (19)$$

This study confirmed that the yield of HNO in reaction (12,13) is large at low pressures. Quantitative comparison with the CH_3ONO measurements awaits characterization of possible wall loss of CHO and CH_3O between the $N_2(A)$ and NO inlet points.

The measured rate constants agree well with those of a previous study,[15] which spanned the pressure range 3 - 190 Torr. Deconvolution of the rate data

to yield rate constants for the recombination (k_{rec}) and atom transfer (k_{AT}) channels (equ. 12 and 13 respectively) is hampered by the fact that the combination channel cannot be assumed to be exhibiting limiting low pressure behavior even at the low pressures of this study. According to Lindemann-Hinshelwood theory, the effective second order rate coefficient, k^{II}, for this channel can be determined, given the limiting low pressure (k_o^{III}) and high pressure (k_∞^{II}) rate constants.

$$k_{rec}^{II} = k_0^{III} k_\infty^{II} [M]/(k_o^{III}[M] + k_\infty^{II}) = k_{LH}, \qquad (20)$$

where M is the buffer gas (Ar or He). However, this theory is oversimple and Troe[16] has suggested an amended expression which yields good agreement, for the fall-off behavior, with RRKM theory. This approach is attractive as, apart from k_∞, the model essentially contains only one variable parameter, S_K, which can be readily estimated from the known fundamental vibration frequencies of CH_3ONO.

Using the measured high pressure rate constant,[15] 1.2×10^{-11} cm^3s^{-1}, for k_∞^{II} and applying this model, values of the rate constants for the two channels were determined by a least squares fit to the rate coefficients at room temperature: $k_{AT} = (2.89 \pm 0.07) \times 10^{-12}$ cm^3s^{-1}, and $k_{rec,0}^{III} = (2.9 \pm 0.3) \times 10^{-29}$ cm^6s^{-1}. In the absence of experimental information, k_∞^{II} was assumed to be independent of temperature and k_o^{III} to vary as T^{-n}. A least squares fit to the complete set of rate data (223 - 473K) yielded $n \sim -2.5 \pm 1.0$. Thus, within the limits of the assumption concerning k_∞^{II}, the following rate constants were derived:

$$k_{rec,0}^{III} = (2.9 \pm 0.3) \times 10^{-29} (T/300)^{-2.5 \pm 1.0} \text{ cm}^6\text{s}^{-1} \qquad (21)$$

$$k_{AT} = (7.9 \pm 1.0) \times 10^{-13} e^{(400 \pm 40)/T} \text{ cm}^3\text{s}^{-1}. \qquad (22)$$

These predict branching fractions for the recombination channel of 0.10 ±

0.02 (297K, 0.5 Torr), 0.17 ± 0.02 (297K, 1.0 Torr) and 0.23 ± 0.06 (223K, 1.0 Torr), in fair agreement with the measured yields of CH_3ONO. At 4.0 Torr and 297K, the predicted HNO branching fraction is 0.65 ± 0.10, in moderate agreement with the uncorrected preliminary value of 0.3 - 0.4.

Previous studies have failed to establish the product distribution principally because CH_3ONO has been employed as the source of CH_3O. For instance, Sanders et al.[17] observed the kinetics of HNO formation to match those of CH_3O removal, whereas Zellner,[15] in a similar experiment, observed CH_2O formation to be limited to the photolysis pulse duration. Thus, while both studies observed HNO + CH_2O formation, the former group ascribed it to a channel of the CH_3O + NO reaction, but Zellner ascribed it to a channel of CH_3ONO photodissociation. Other investigations employed steady-state photolysis or thermal dissociation of CH_3ONO and are less direct; however, these found a small branching fraction of 0.10 - 0.15 for reaction (13) at high pressures.

The present study has demonstrated clearly that atom transfer is the major channel at low pressure. The inverse temperature dependence for this channel (which is evident from Fig. 3 and is independent of the way in which the recombination channel is modeled) suggests strongly that this channel occurs mainly via decomposition of the energetic CH_3ONO intermediate rather than via direct abstraction of a H atom. Thus, the rate coefficient for this channel should become smaller at high pressure, because of competitive collisional stabilization of the intermediate. Our findings are qualitatively in agreement with previous studies. A more quantitative comparison could be achieved by RRKM calculations which, however, require considerable information concerning the potential energy surface for this reaction.

6. The Reactions of CH_3O with O and H atoms.

This project is continuing beyond the end of this grant period. Although the results are incomplete, they are sufficiently interesting to warrant this brief report. Radical-radical reactions, involving carbonaceous species, are expected to occur at close to the collision rate and they may be important in combustion systems. The reactions of CH_3O with H and O atoms may occur via strongly-bound intermediates and have available more than one reaction channel:

$$CH_3O + O \rightarrow CH_3O_2 \quad (23)$$

$$\rightarrow CH_3 + O_2 \quad (24)$$

$$\rightarrow CH_2O + OH \quad (25)$$

$$CH_3O + H \rightarrow CH_3OH \quad (26)$$

$$\rightarrow CH_2OH + H \quad (27)$$

$$\rightarrow CH_2O + H_2 \quad (28)$$

$$\rightarrow CH_3 + OH. \quad (29)$$

CH_3O is produced by reaction of F with CH_3OH, using a discharge through dilute mixtures of F_2 or CF_4 in He as the source of the F atoms. CH_3O is monitored by LIF. O or H atoms are produced in excess by discharging respectively O_2 or H_2. The absolute O-atom concentration is measured via O + NO chemiluminescence, calibrated via the O + NO_2 titration technique. The absolute H atom concentration is measured by chemical conversion to OH, which is detected by resonance fluorescence.

In the initial stage of this investigation, the rate constants of the

reactions of CH_3O with H and O at room temperature have been investigated. In both reactions, care has to be taken to achieve accurately exponential decays of the minor species CH_3O as a function of reaction time. In the H-atom reaction, this was achieved by adding excess H_2, presumably to remove any remaining (or newly-formed) F atoms in the reaction zone. Typical CH_3O decays are shown in Figure 9; the preliminary rate constant is $\sim 1 \times 10^{-10}$ cm^3s^{-1}, three times larger than a previous estimate,[18] and only a factor of three below the collision rate. This rate constant is too high for combination, equ. (26), to be the major channel; the branching between the other channels is clearly of interest.

In the reaction of CH_3O with O atoms, our preliminary rate constant is 3 to 10 times <u>smaller</u> than the previous measurement[19] of 3×10^{-11} cm^3s^{-1}. Because of the rapidity of the $CH_3O + H$ reaction, careful modeling of the reaction with O will be required, because of the possible reaction sequence:

$$CH_3O + O \rightarrow CH_3 + O_2 \quad (30)$$

$$\rightarrow OH + CH_2O \quad (31)$$

$$CH_3 + O \rightarrow CH_2O + H \quad (32)$$

$$OH + O \rightarrow O_2 + H, \quad (33)$$

followed by reaction of CH_3O with H. Clearly, the most reliable data will be expected at large initial $[O]/[CH_3O]$ concentration ratios. In the continuation of this study, rate constants over a range of temperature and carrier gas pressure will be determined, and the product channels will be investigated.

References

1. J. A. McCaulley, S. M. Anderson, J. B. Jeffries, and F. Kaufman, Chem. Phys. Lett. 115 180 (1985).
2. K-J. Hsu, J. L. Durant and F. Kaufman, J. Phys. Chem. 91 1895 (1987).
3. J. B. Jeffries, J. A. McCaulley and F. Kaufman, Chem. Phys. Lett. 106 111 (1984).
4. U. C. Sridharan, L. X. Qiu and F. Kaufman, J. Phys. Chem. 86 4569 (1982).
5. M. A. A. Clyne and B. A. Thrush, Proc. Roy. Soc. A275 559 (1963).
6. A. A. Westenberg and N. de Haas, J. Phys. Chem. 76 1586 (1972).
7. J. J. Ahumada, J. V. Michael and D. T. Osborne, J. Chem. Phys. 57 3736 (1972).
8. M. W. Slack, Comb. Flame 28 241 (1977).
9. G. Dixon-Lewis and A. Williams, 11th Symposium (International) on Combustion, the Combustion Institute, 1967, p. 951.
10. R. W. Getzinger and L. S. Blair, Comb. Flame 13 271 (1969).
11. T. Khatoon and K. Hoyermann, Ber. Bunsenges, Phys. Chem. 92 669 (1988).
12. D. J. Bogan, W. A. Sandes, H. G. Eaton and M. J. Kaufman, 7th International Symposium on Gas Kinetics, A35, Göttingen, 1982.
13. J. A. McCaulley, N. Kelly, M. F. Golde and F. Kaufman, J. Phys. Chem., in press.
14. W. Tao, M. F. Golde, G. H. Ho and A. M. Moyle, J. Chem. Phys. 87 1045 (1987).
15. R. Zellner, J. Chim. Physique, to be published.
16. J. Troe, Ber. Bunsenges Phys. Chem. 78 478 (1974).
17. N. Sanders, J. E. Butler, L. R. Pasternak and J. R. McDonald, Chem. Phys. 48 203 (1980).

18. K. Hoyermann, N. S. Loftfield, R. Sievert and H. Gg. Wagner, 18th Symp. Comb., The Combustion Institute, 1981, p. 831.

19. F. Ewig, D. Rhasa and R. Zellner, Ber. Bunsenges. Phys. Chem. 91 708 (1987).

20. R. G. MacDonald, J. J. Sloan and P. T. Wassell, Chem. Phys. 41 201 (1979).

21. B. Dill and H. Heydtmann, Chem. Phys. 54 9 (1980).

22. U. Meier, H. H. Grotheer and Th. Just, Chem. Phys. Lett., 106 97 (1984).

23. M. A. Wickramaaratchi, D. W. Setser, H. Hildebrandt, B. Korbitzer and H. Heydtmann, Chem. Phys. 95 109 (1985).

Table 1: Methoxy yield of the F + methanol reaction

Reagent	Method[a]	$f_{CH_3O(CD_3O)}$	Reference
CH_3OD	HF,DF; IRCL	0.50	20
CH_3OD	HF,DF: IRCL	0.31 ± 0.03	21
CH_3OD	HF,DF; MS	0.3 ± 0.1	18
CD_3OH	HF,DF; MS	0.5 ± 0.2	18
CH_3OH	CH_2OH; MS	0.59 ± 0.06	22
CH_3OD	HF,DF; IRCL	0.38 ± 0.24	23
CD_3OH	HF,DF; IRCL	0.63 ± 0.07	23
CH_3OH	MS	0.60	11
CH_3OD	MS	0.63	11
CD_3OH	MS	0.61	11
CD_3OD	MS	0.64	11
CH_3OD	HF,DF; MS	0.81 ± 0.07	this work
CD_3OH	HF,DF; MS	0.69 ± 0.08	this work

a. Methods: IRCL, infrared chemiluminescence; MS, mass spectrometry.

Table 2: Second-order rate coefficients of hydroxyl + methanol reactions

T = 298 ± 2 K p = 3.00 ± 0.05 Torr

Reaction	$\bar{v}$, a cm s^{-1}	#b		10^{13} k^{II}, cm^3 s^{-1}
OH + CH_3OH	931	6		9.7 ± 1.4
"	949	8		10.5 ± 1.5
"			AVE	10.1 ± 1.0
OD + CH_3OH	549	8		9.5 ± 1.2
OD + CH_3OD	468	8		9.3 ± 1.1
OH + CD_3OH	449	14		3.35 ± 0.72
OD + CD_3OH	449	8		2.86 ± 0.37
OH + CD_3OD	951	8		1.34 ± 0.15
"	979	5		1.72 ± 0.21
"	463	6		2.22 ± 0.40
"	444	5		2.22 ± 0.30
"	674	9		2.16 ± 0.28
"			AVE	1.93 ± 0.45
OD + CD_3OD	463	7		1.80 ± 0.33
"	444	8		1.57 ± 0.23
"	675	5		1.64 ± 0.23
			AVE	1.67 ± 0.16

a. average bulk flow velocity
b. number of methanol concentrations

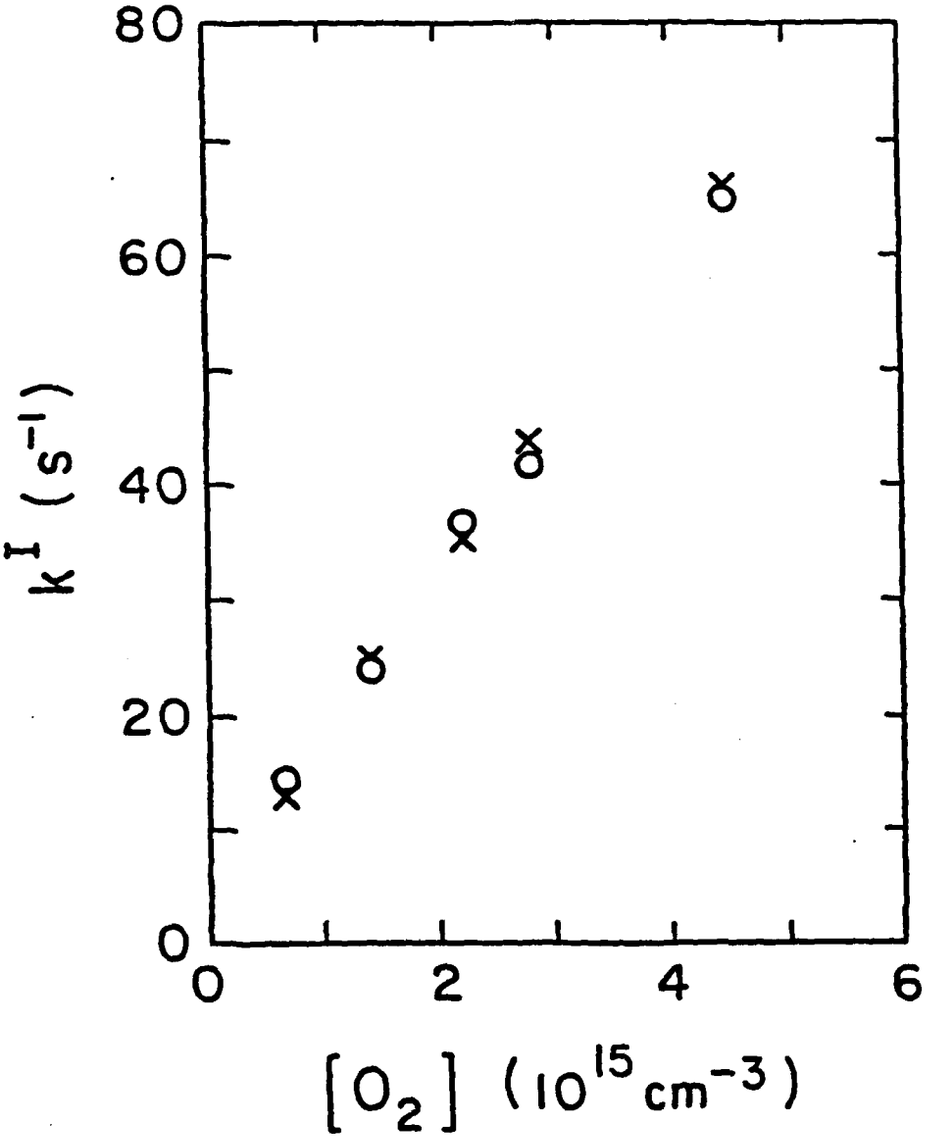

Figure 1 Plot of Pseudo-First Order Rate versus $[O_2]$ for the Reaction H + O_2 + M at 5.3 torr. (He: 40.8%, N_2: 59.2%), O: experimental, x: calculated; k_{slope}= 1.3×10^{-14} $cm^3 s^{-1}$, $k_{calc.}$= 0.99×10^{-14} $cm^3 s^{-1}$.

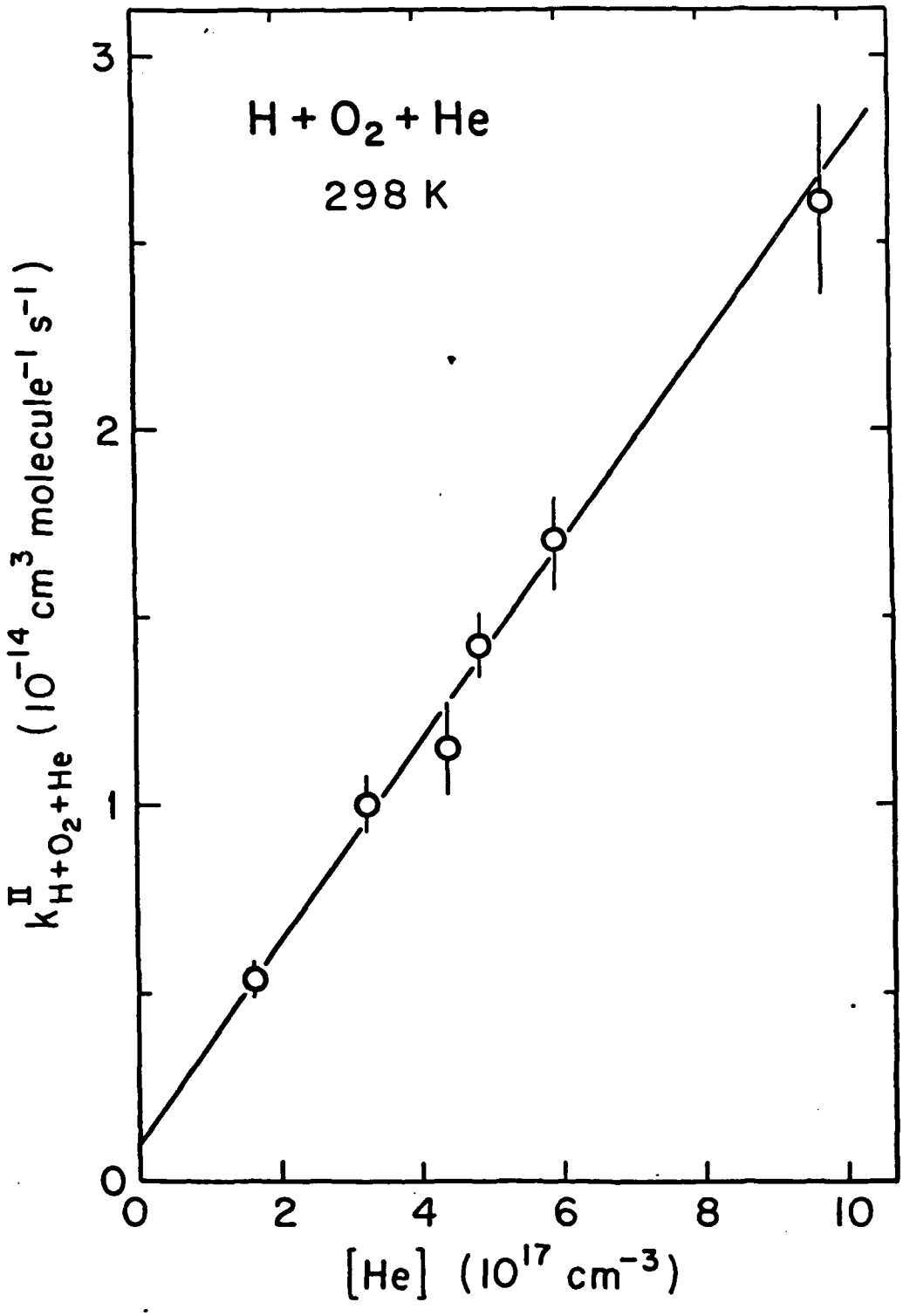

Figure 2. Plot of Pseudo-Second Order Rate Constant versus Helium Concentration at 298K.

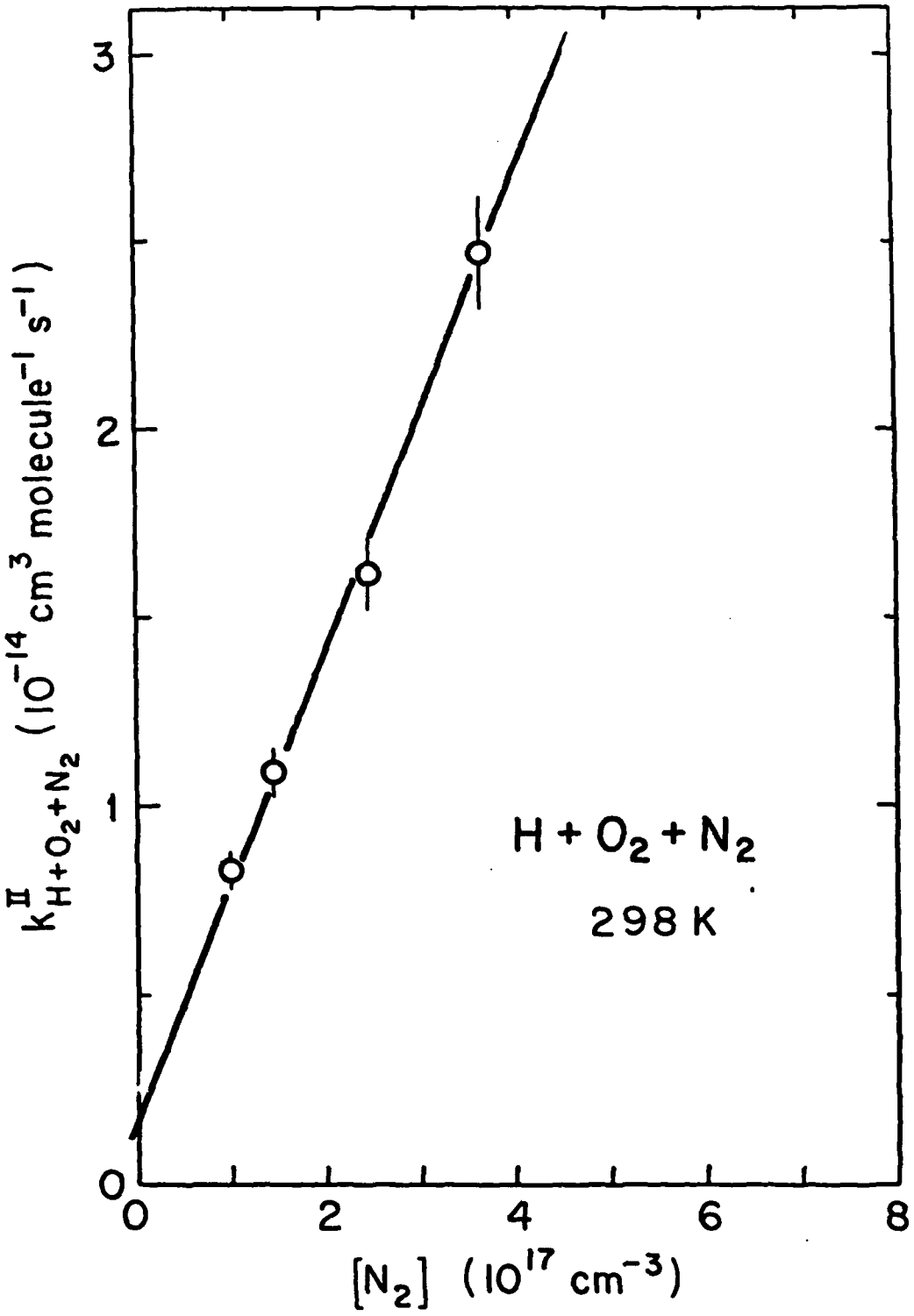

Figure 3. Plot of Pseudo-Second Order Rate Constants versus N_2 Concentrations for the Reaction H + O_2 + N_2 at 298K.

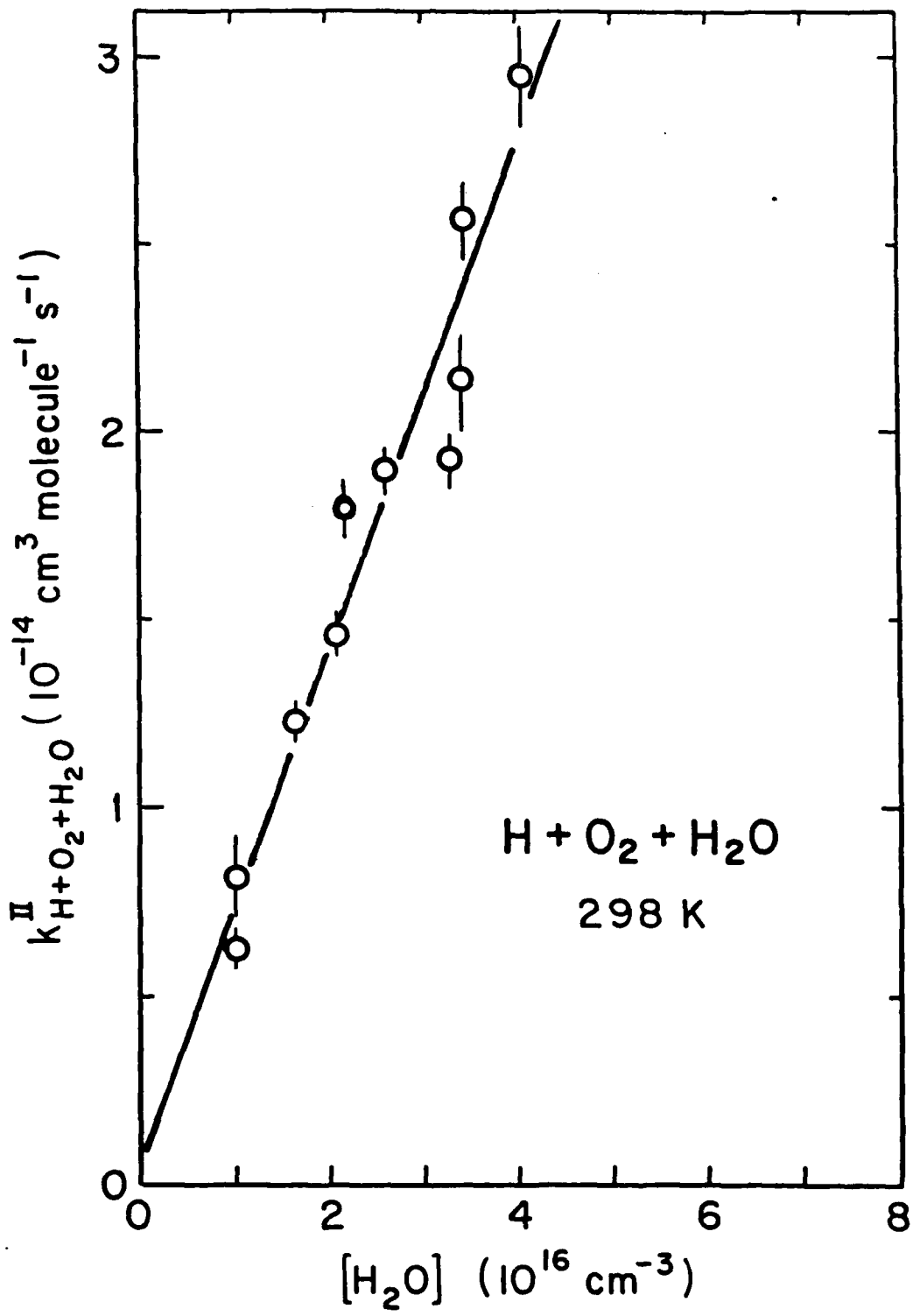

Figure 4. Plot of Pseudo-Second Order Rate Constant versus H_2O Concentrations for the Reaction $H + O_2 + H_2O$ at 298 K.

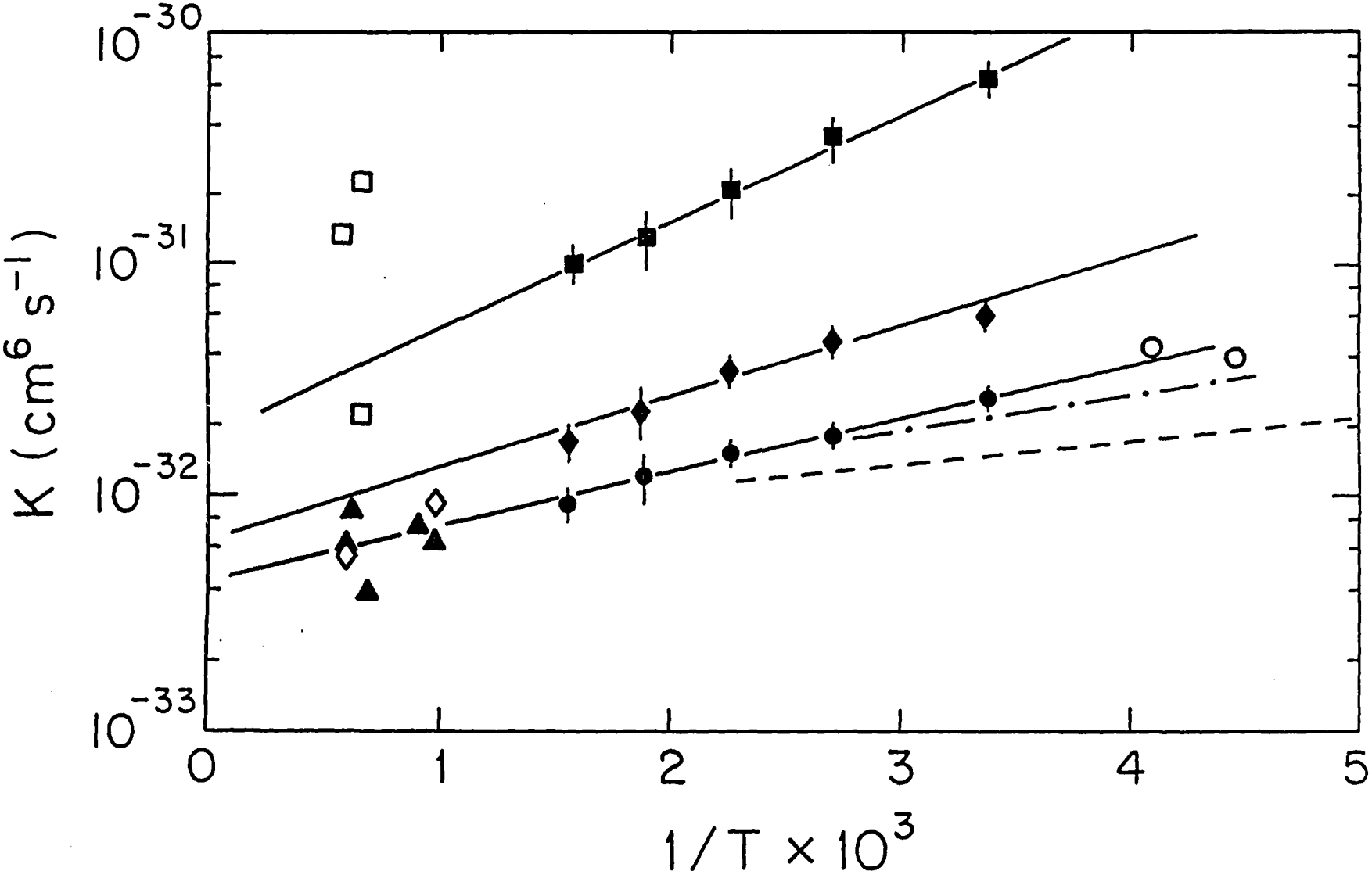

Figure 5. Arrhenius plot for H + O_2 + M third-order rate constants.
Third body: △ Ar, ○ He, ◇ N_2, □ H_2O

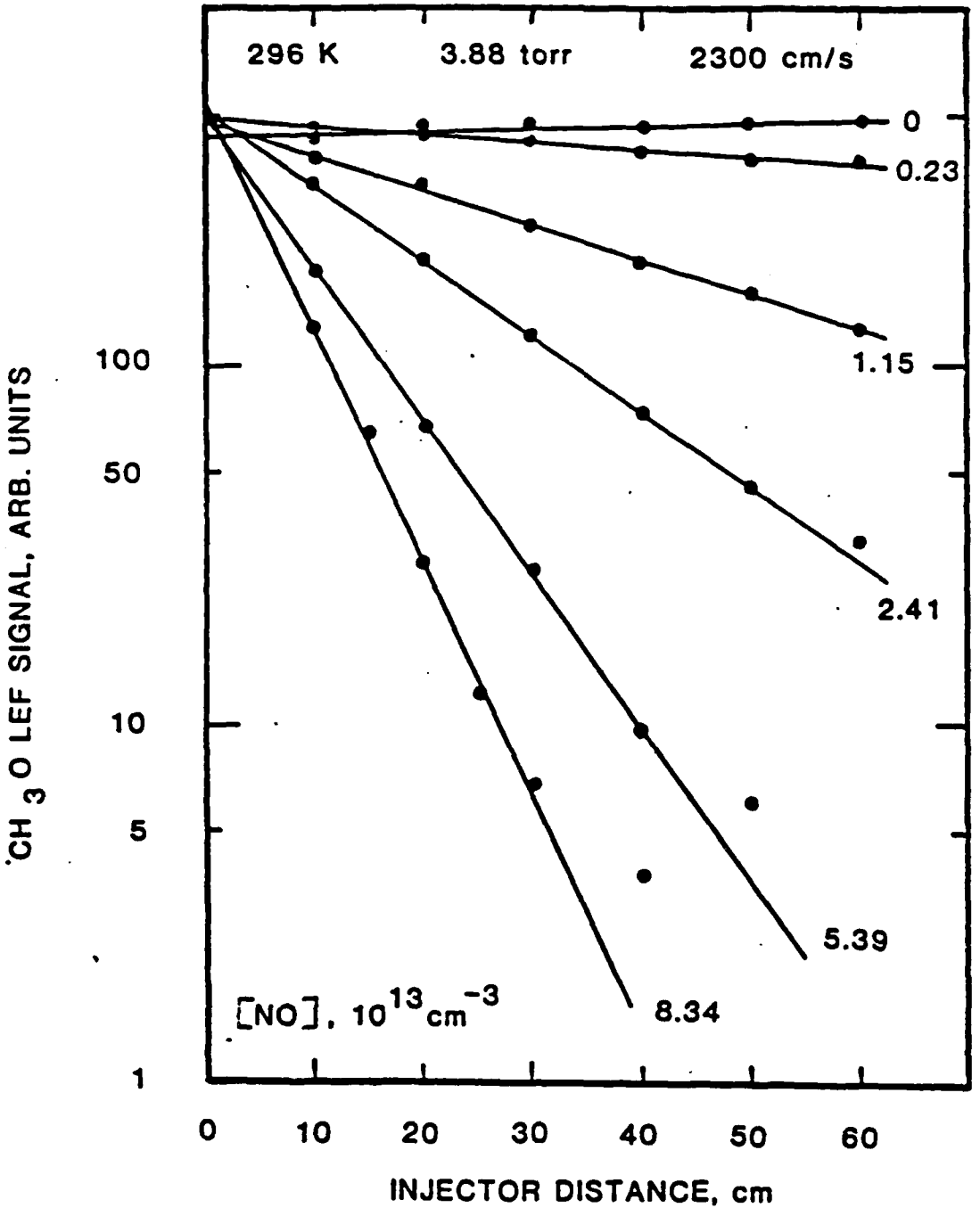

Figure 6. CH_3O + NO: decay plots with curvature attributed to CH_3O self-reaction

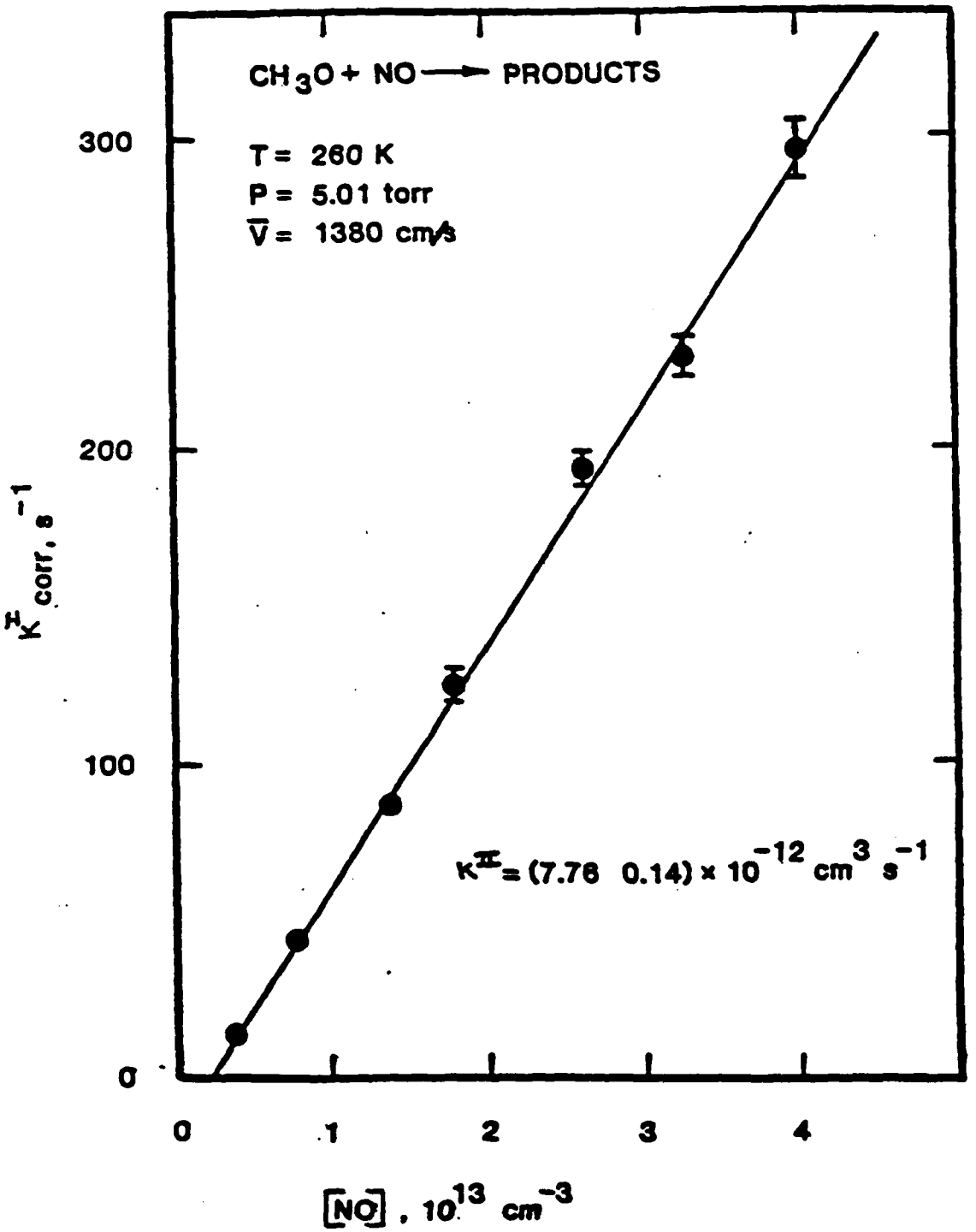

Figure 7. $CH_3O + NO$: k'_{corr} vs [NO]

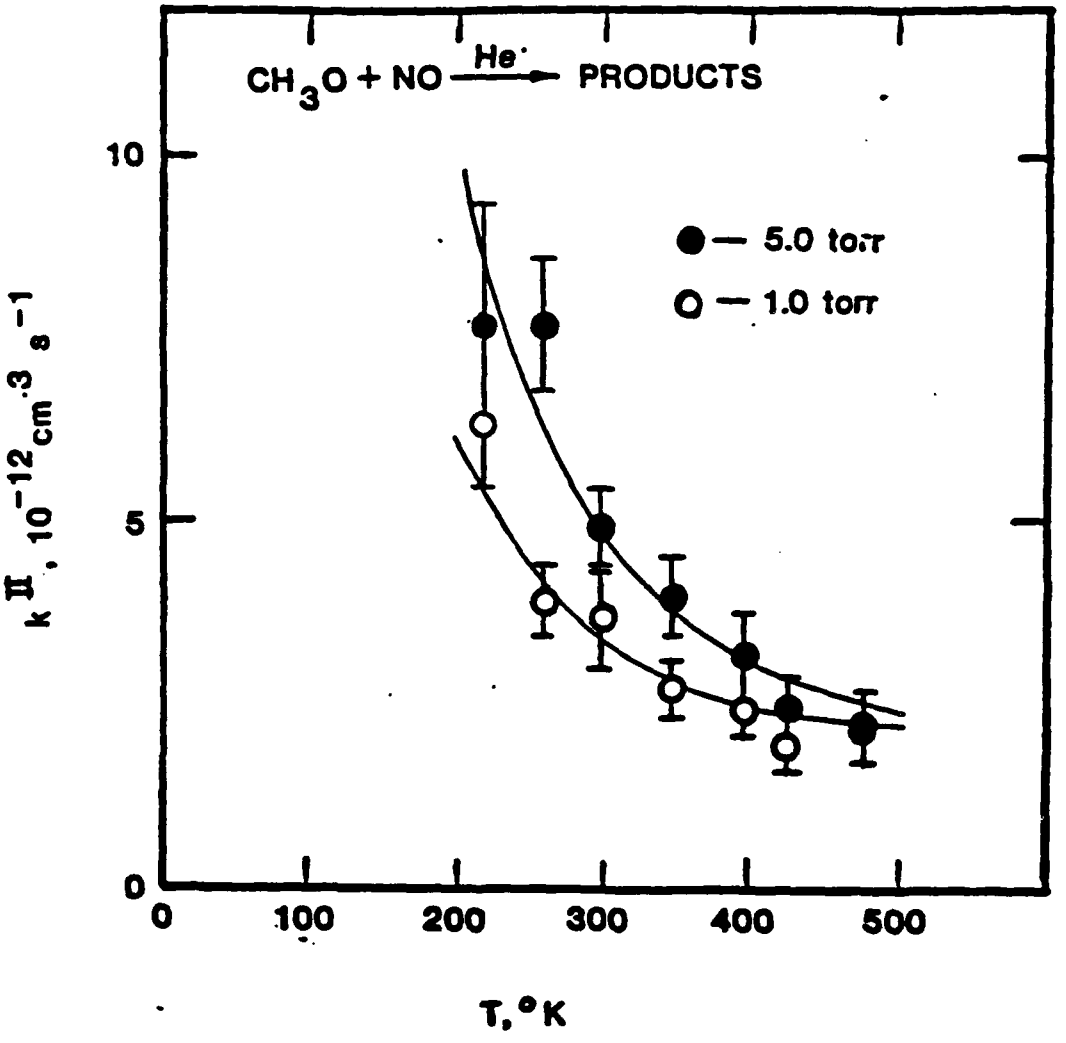

Figure 8. CH_3O + NO: pressure and temperature dependence of k^{II}

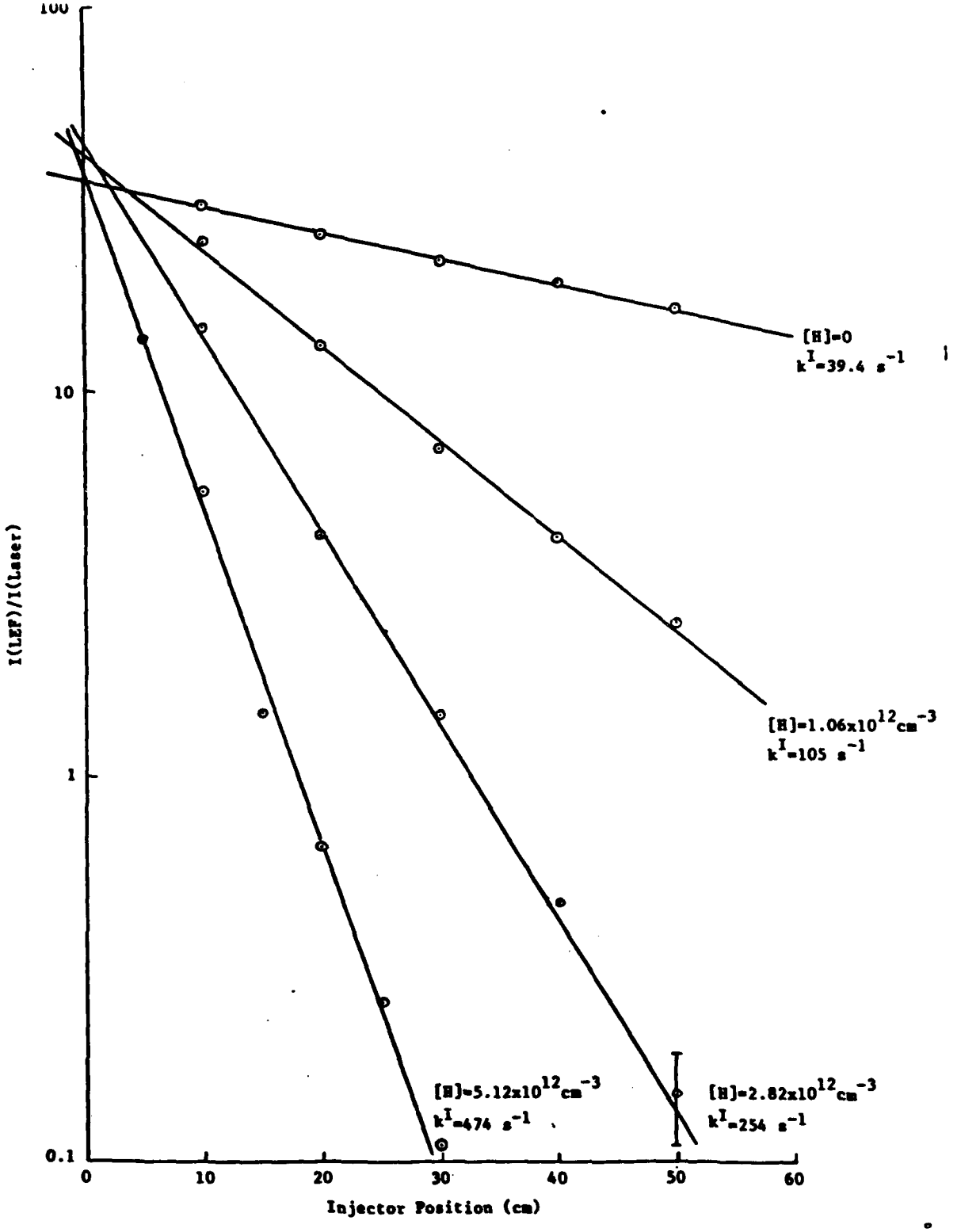

Figure 9. CH_3O + H: decay curves

Publications under ARO Sponsorship

1. F. Kaufman, Rates of Elementary Reactions: Measurement and Applications, Science 230 393 (1985).
2. S. M. Anderson, F. S. Klein and F. Kaufman, Kinetics of the Isotope Exchange Reaction of ^{18}O with NO and O_2 at 298K, J. Chem. Phys. 83 1648 (1985).
3. K-J. Hsu, J. L. Durant and F. Kaufman, Rate Constants for H + O_2 + M at 298K for M = He, N_2 and H_2O, J. Phys. Chem. 91 1895 (1987).
4. J. L. Durant and F. Kaufman, Calculation and Use of Total Collision Rates in Thermal Systems, Chem. Phys. Lett. 142 246 (1987).
5. J. A. McCaulley, N. Kelly, M. F. Golde and F. Kaufman, Kinetic Studies of the Reactions of F and OH with CH_3OH, J. Phys. Chem., in press (F. Kaufman Memorial Issue).
6. K-J. Hsu, S. M. Anderson, J. L. Durant and F. Kaufman, Rate Cosntants for H + O_2 + M from 298 to 639K for M = He, N_2 and H_2O, J. Phys. Chem., in press (F. Kaufman Memorial Issue).
7. J. A. McCaulley, A. M. Moyle, M. F. Golde and F. Kaufman, Kinetics of the Reaction of CH_3O with NO, in preparation.